MINIREVIEW

Visualizing Protein-Protein Interactions in the Nucleus of the Living Cell

Richard N. Day, Steven K. Nordeen, and Yihong Wan

Departments of Medicine and Cell Biology (R.N.D.)
National Science Foundation Center for Biological Timing
University of Virginia Health Sciences Center
Charlottesville, Virginia 22908

Department of Pathology and Program in Molecular Biology
University of Colorado Health Sciences Center
Denver, Colorado 80262

INTRODUCTION

A question of central importance to the molecular endocrinologist is how hormones function to orchestrate events within cells. The cascades of cellular responses that are triggered by endocrine signals require the formation of specific protein partnerships, and these protein-protein interactions must be coordinated in both space and time. For example, in the absence of ligand, the steroid hormone receptor for estradiol is associated with a multiprotein inhibitory complex (1). The binding of estradiol results in alterations in estrogen receptor conformation that allow it to dissociate from this complex, and the receptor becomes competent to interact with specific DNA elements in the regulatory regions of target genes. The efficient utilization of these regulatory elements by the receptor, however, requires that the receptor associate with other coregulatory proteins (2–4). Biochemical approaches such as coimmunoprecipitation and Far-Western blotting and *in vivo* approaches such as yeast two-hybrid assay have provided important information regarding the interactions between receptors and coregulatory proteins. These approaches, however, may sometimes implicate nonphysiological associations between proteins that do not normally occur in intact cells. Deciphering where and when specific protein partnerships form within the living cell will be critical to understanding these basic cellular events.

The molecular cloning of the jellyfish green fluorescent protein (GFP) and its expression in a variety of cell types have had a major impact on our ability to monitor events within living cells (5–10). GFP retains its fluorescent properties when fused to other proteins, and this allows fluorescence microscopy to be used to monitor the dynamic behavior of the expressed GFP fusion proteins in their natural environment within the living cell. There are now many examples of proteins expressed as GFP chimeras that possess the same subcellular localization and biological function as their endogenous counterparts. For example, the dynamics of nuclear translocation for the glucocorticoid (11, 12) and androgen receptors (13) have been visualized using GFP fusions. GFP fusion proteins have also been used to monitor complex cellular events such as the sorting of proteins between organelles (14) and the dynamics of regulated protein secretion (15, 16). Recently, it was demonstrated that movement of β-arrestin2-GFP fusion proteins serves as a sensitive biosensor for G protein-coupled receptor activation (17). This illustrates the potential for GFP fusion proteins to act as indicators of many different intracellular events.

Mutant forms of the GFP protein that emit lights of different colors have been generated that, when coexpressed in the same cell, can be readily distinguished by fluorescence microscopy. This allows the behavior of two independent proteins to be monitored in the intact cell, and the extent to which these proteins colocalize can be assessed. To determine whether these labeled proteins are physically interacting, however, would require resolution beyond the optical limit of the light microscope. Fortunately, this degree of spatial resolution can be achieved with the conventional light microscope using the technique of fluorescence resonance energy transfer (FRET). FRET microscopy involves the detection of increased (sensitized) emission from an acceptor fluorophore that occurs as the result of the direct transfer of excitation energy from an appropriately positioned fluorescent

0888-8809/99/$3.00/0
Molecular Endocrinology

donor. The efficiency of energy transfer from the donor to the acceptor is extremely sensitive to the distance between the fluorophores and is limited to the scale of nanometers (18). As will be discussed below, the spectral characteristics of some of the mutant variants of GFP allow them to be used as donor and acceptor pairs for FRET microscopy.

The expression of nuclear proteins fused to color variants of GFP provides a method to visualize where and when two independent nuclear proteins localize within the nuclear compartment of intact cells. When combined with FRET microscopy, this approach has the potential to report dynamic changes in protein-protein interactions as they occur in the nucleus. These types of studies will complement the biochemical and two-hybrid experimental approaches and will have important implications for understanding the mechanisms underlying gene regulation. In this paper, we review the characteristics of the GFPs that make them useful for the study of nuclear protein behavior in living cells.

CHARACTERISTICS OF THE GFPs

The jellyfish GFP is a 27-kDa protein that absorbs near-UV light and emits green light. GFP owes its fluorescent properties to a chromophore that forms by a posttranslational oxidation and cyclization reaction involving the tripeptide sequence, Ser^{65}, Tyr^{66}, Gly^{67} (19–22). The crystal structure of GFP reveals an 11-stranded β-barrel cylinder surrounding the central chromophore (23). Because the protein must fold into this barrel structure for appropriate formation of the chromophore, nearly the entire 238-amino acid sequence is necessary for fluorescence (24). In addition, the formation of the chromophore is a relatively slow process requiring several hours (25, 26). Therefore, it is critical that protein fusions to GFP do not interfere with the ability of the chromophore to form and, when imaging newly synthesized GFP fusion proteins, it is important to consider the rate of chromophore formation.

The major limitation to the detection of GFP in living cells is the autofluorescent background. For cells grown as a monolayer in culture, this background is primarily due to intracellular NAD(P)H, riboflavin, flavin coenzymes, and flavoproteins bound in the mitochondria (27). In more complex cell cultures, such as slice preparations from transgenic animal tissues, certain specialized structures may contribute significantly to this fluorescent background (28). The autofluorescent signal can be substantial at near-UV wavelengths, and this has limited the detection of wild-type GFP (wtGFP) to approximately 10^5 molecules per cell (7). Fortunately, mutagenesis of the wtGFP protein sequence has generated variant forms with increased brightness and differing spectral characteristics (19, 23, 25, 29). A mutation changing the chromophore Ser^{65} to threonine (GFP^{S65T}) resulted in a shift in excitation away from the near-UV to a peak at 489 nm and yielded a 4- to 6-fold improvement in the intensity of green light emission when compared with wtGFP (25). Improvements in the expression of GFP^{S65T} in mammalian cells was obtained by optimizing codon usage to facilitate its translation (30–32) and by the introduction of mutations that enhance protein folding at 37 C (33, 34). Taken together, these mutations have dramatically improved the fluorescence signal obtained from GFP chimeras, allowing the detection of fewer than 10,000 GFP molecules in single living cells (26).

Mutations within the chromophore have also produced several color variants of GFP. For example, changing Tyr^{66} to His resulted in a blue fluorescent protein (BFP) that, when excited by UV light, has a peak emission at 445 nm (19, 29). BFP is more difficult to detect than the GFP variants, however, because of its low quantum yield and sensitivity to photobleaching. Other GFP variants with emission wavelengths from cyan (greenish blue) to yellowish green have been isolated (23, 29), and these may prove more useful than BFP and GFP^{S65T} for some applications. However, because the peak emission values for BFP and GFP^{S65T} are substantially different (445 nm and 511 nm, respectively), BFP has utility when used in conjunction with GFP^{S65T} as a second protein tag (Refs. 35 and 36; see below).

PROTEIN FUSIONS TO THE GFPs

Plasmid vectors encoding several of the color variants of GFP that have been optimized for expression in mammalian cells are commercially available. These vectors allow for fusion of GFP to any cloned gene of interest, and standard gene transfer techniques are used to introduce these vectors into cells for the expression of the chimeric proteins. The detection of GFP fusion proteins does not require the addition of substrates or the permeabilization and fixation of cells. This improves the sensitivity and reduces the potential for artifacts associated with immunohistochemical approaches (37). The primary consideration in the generation of GFP fusion proteins is functionality, both of the fluorescent protein tag and the protein of interest. As mentioned above, the GFPs must fold correctly when positioned at either the amino- or at the carboxy-terminal end of the protein of interest. Equally important is that the protein being studied retains its normal cellular function when fused to the 27-kDa fluorescent protein. Therefore, it is critical that the expressed fusion proteins be tested for function by as many independent methods as possible. For example, fluorescence microscopy of transiently transfected cells will show that the GFP chimeras are being expressed, reveal their subcellular localization, and indicate the level of the GFP signal over the autofluorescence background. Confirmation that the expressed

fusion proteins are full length is then obtained by Western blotting of proteins extracted from the transfected cells. Antisera directed against the protein of interest and against GFP can be used sequentially to identify the expressed protein. Antibodies for detection of GFP that are suitable for Western analysis are commercially available. Further, it is important to identify a method that directly demonstrates that protein function is not impaired by the GFPs. For example, GFP fusions to transcription factors can be tested for binding to appropriate DNA elements using electrophoretic mobility shift assay, and their ability to influence specific gene transcription can be determined in reporter gene studies (38). A more rigorous demonstration of GFP chimera function is the capacity of the fusion protein to rescue a mutant phenotype in a transgenic organism. For example, Take-Uchi and colleagues (39) recently showed that expression of a GFP-sodium channel fusion protein in a mutant strain of *Caenorhabditis elegans* could reestablish a complex rhythmic behavior.

CONSIDERATIONS FOR IMAGING PROTEINS FUSED TO THE GFPs

The coexpression of BFP- and GFP^{S65T} fusion proteins, combined with dual channel fluorescence microscopy, provides a method for monitoring the intracellular trafficking of two independent proteins in the same cell (35, 36). When GFP chimeras are imaged in intact cells, there are several important considerations that become especially relevant when using dual-channel fluorescence microscopy. The choice of the basic components of a fluorescence microscope system, including the excitation source, objective lenses, filters, and detector, has important consequences for image quality. For example, a mercury lamp gives off light concentrated at certain wavelengths, and its bright blue lines of emission are ideal for excitation of GFP. However, a xenon lamp, with its spectrally uniform profile from the UV to far red, may be preferable for excitation of BFP and for studies involving the imaging of two different color fluorophores. Moreover, efficient excitation at near UV-wavelengths requires the use of optics that are specifically designed to transmit UV light. It is also important to recognize that color-dependent distortions in the image can arise when fluorescence signals at two different wavelengths are projected to the detector with different efficiencies. This chromatic aberration is largely corrected for in high-quality imaging systems that use uniform illumination of the specimen and matched apochromatic optics (40).

The efficiency of light collection (*i.e.* the brightness of the fluorescence signal) and the ability to resolve objects are both functions of the numerical aperture (NA) of the objective lens. The selection of a higher NA objective lens (*e.g.* NA 1.4) will increase the amount of light captured to the detector and improve image resolution and contrast. However, resolution can be lost to spherical aberration of the objective lens that occurs when light from the center of the specimen is focused differently than that coming from the periphery. Most objectives are corrected for spherical aberration, but this correction requires a constant refractive index in the light path. Therefore, a high NA oil-immersion objective that works well for fixed samples in mounting media will be less than optimal for imaging living cells in aqueous culture media. Recently, high-NA water-immersion objectives have become available that greatly improve the contrast and resolution of images obtained from living cell preparations.

Appropriate filters are required to discriminate the blue light emission of BFP from the green light emission of GFP^{S65T}. Because the cellular autofluorescence signal has a wide spectrum, narrow bandpass emission filters will improve the discrimination of fluorescence signals above the background, but will also reduce the overall signal. Moreover, due to the broad nature of the excitation and emission spectra for the BFP and GFP^{S65T} variants (29), it is important to select an excitation filter for BFP that has a minimal coincidental excitation of GFP^{S65T}. Filter sets that are designed specifically for the detection of the different color variants of GFP are now commercially available. Finally, the low quantum yield of BFP and its susceptibility to photobleaching create additional challenges for its detection above the background noise. Because BFP and GFP^{S65T} bleach at very different rates, the images acquired using dual channel will reflect the illumination history of the cell. It is therefore important to use a detector with maximal sensitivity at blue and green wavelengths to minimize the intensity and duration of exposure to the excitation light that is required for detection of BFP fusion proteins. Because of their sensitivity and linear response, charge-coupled device (CCD) digital cameras are typically used in conventional fluorescence microscopy. The cameras with the highest sensitivity are cooled to minimize dark charge noise and use back-illuminated sensors that bring light directly to the photosensitive CCD (41).

DUAL CHANNEL IMAGING OF NUCLEAR PROTEINS FUSED TO THE GFPs

It is becoming increasingly clear that transcription factors are localized to specific domains within the nucleus (42). The steroid hormone receptors, for example, appear to be highly regulated in their intranuclear pattern of distribution (43–45). Dual-channel fluorescence microscopy of cells coexpressing nuclear proteins fused to the BFP- and GFP^{S65T} spectral variants allows the visualization of the patterns of distribution for two different proteins within the nuclei of living

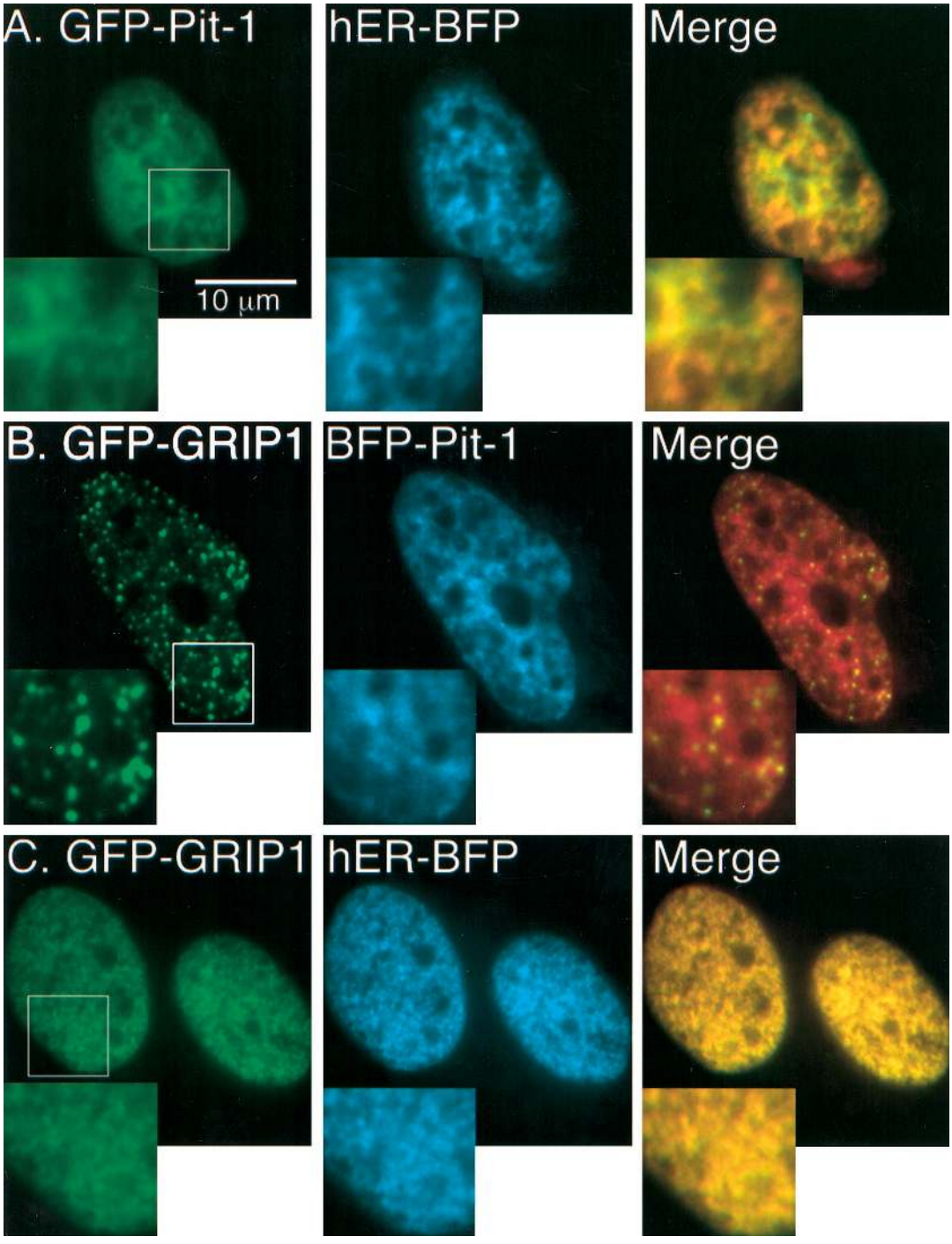

Fig. 1. Comparison of the Nuclear Distribution for Pit-1, Human Estrogen Receptor (hER), and Coactivator GRIP1

Methods: HeLa cells were transfected with expression vectors encoding the indicated fusion proteins by electroporation and used to inoculate cultures on 25-mm coverglass. The cultures were maintained in medium supplemented with 10% newborn calf serum containing endogenous estrogens overnight at 33 C and then transferred to 37 C. The fluorescence images were acquired with a 60× aqueous-immersion objective lens using a 100 W mercury-xenon arc lamp excitation light source. The filter combinations were 485/22 nm excitation and 535/50 nm emission for GFP images; 365/15 nm excitation and 460/50 nm emission for BFP images. Grayscale images of the cells were obtained using a cooled CCD camera with digital output of 1317 × 1035 pixels with 12 bits resolution. The images were converted to RGB assigning GFP images to the *green* channel and BFP images to the *blue* channel. The digital images were then merged by assigning the GFP image to the *green* channel and the corresponding BFP image to the *red* channel of the same image. A, Images of the nucleus of a HeLa cell coexpressing GFP-Pit-1 (*left, scale bar* indicates 10 μm) and hER-BFP (*middle*), the *inset* is the enlarged area indicated by the *square in the left panel*. The GFP and BFP images were merged as described above to show regions of overlap (indicated by *yellow*) and regions where hER-BFP and GFP-Pit-1 are distinct in their localization (indicated by *red* or *green* in merged images, *right*). B, Images of the nucleus of a HeLa

cells. Here we demonstrate this approach by comparing and contrasting the subnuclear localization pattern of the homeodomain transcription factor Pit-1, the human estrogen receptor (hER), and the coactivator glucocorticoid receptor-interacting protein (GRIP1). GRIP1 is the mouse homolog of the nuclear receptor coactivator TIF2 that interacts directly with the ligand-binding domain of several different nuclear receptors (46, 47). The results shown in Fig. 1 illustrate how signals originating from cells coexpressing pairs of these nuclear proteins tagged with the GFP or BFP variants can be discriminated by dual-channel fluorescence microscopy. In Fig. 1A, this approach is used to acquire gray-scale images of a HeLa cell coexpressing GFP-Pit-1 and hER-BFP. The images acquired for each fluorophore are converted to red-green-blue (RGB) images, using the green channel to indicate GFP and the blue channel to indicate BFP. The individual GFP and BFP images from the same cell are then merged into a single RGB image to assess the overlap in the subnuclear localization of the labeled proteins. For this application the GFP image is again assigned to the green channel, but the BFP image is now assigned to the red channel of the same image. In this way, signals from colocalized proteins appear as yellow in the merged image, whereas nonoverlaping signals remain green and red. In the case shown in Fig. 1A for a HeLa cell coexpressing GFP-Pit-1 and hER-BFP, the merged image reveals areas of overlap (indicated by *yellow* in merged images, panel A) as well as regions where hER-BFP and GFP-Pit-1 are distinct in their localization (indicated by *red* in merged images, panel A). An even more striking example of different localization patterns is observed for cells coexpressing GFP-GRIP1 and BFP-Pit-1 (Fig. 1B). The distribution of GFP-GRIP1 in the nucleus of the HeLa cell shown in Fig. 1B is distinct from the pattern observed for the coexpressed BFP-Pit-1 protein (merged image, panel B). In marked contrast, when GFP-GRIP1 and hER-BFP are coexpressed in HeLa cells, we observe identical patterns of nuclear distribution (Fig. 1C). The targeting of the fluorescently labeled estrogen receptor and GRIP1 proteins to the same subnuclear sites could potentially function to facilitate interactions between these proteins *in vivo*. Evidence for a functional interaction between GRIP1 and the estrogen receptor comes from the observation that GRIP1 potentiates receptor-mediated transcription, and physical interactions were indicated *in vitro* by coimmunoprecipitation studies (48). What is needed, however, is a direct demonstration of physical interactions between these proteins in the living cell. The colocalization studies shown here are limited by the optical resolution of the light microscope and can only indicate proximity on the scale of approximately 0.25 μm (2,500 Å). To determine whether these labeled proteins are physically interacting requires resolution beyond the optical limit of the light microscope. This degree of spatial resolution can be achieved by conventional light microscopy using the technique of FRET microscopy.

FRET MICROSCOPY TO VISUALIZE PROTEIN INTERACTIONS

FRET microscopy detects the fluorescence emission from acceptor fluorophores that results from the direct transfer of excitation energy from appropriately positioned donor fluorophores. This requires that there be a substantial overlap in the emission spectrum of the donor with the absorption spectrum of acceptor, and some of the GFP color variants have the required spectral overlap. For example BFP can donate excitation energy to GFP^{S65T} (29, 49, 50), and the cyan color variant can serve as a donor for the yellowish mutant (51). Because the efficiency of energy transfer varies inversely with the sixth power of the distance separating the donor and acceptor fluorophores, FRET can only occur over a distance limited to approximately 20–100 Å (29, 51). To put this in perspective, the ribosome, a complex of 60 proteins and RNA molecules, is approximately 300Å across, and the light microscope could resolve ribosomes clustered in groups of seven or more. In contrast, the detection of sensitized fluorescence emission by FRET microscopy reveals that the distance separating proteins labeled with the color variants of GFP is on the order of 20–100 Å, the diameter of a single globular protein that is part of the ribosome complex. Before the development of the spectral variants of GFP, the application of FRET to living cells was limited to fluorescent probes directed to the cell surface (52, 53) or to those microinjected into individual cells (54). Now FRET microscopy can potentially detect interactions between any proteins that retain biological function when expressed as a fusion to the GFPs.

Two distinct approaches that take advantage of the combination of the GFPs and FRET imaging have recently been used to monitor intracellular events. The first approach involves the detection of intramolecular FRET signals that originate from chimeric proteins containing donor (BFP or the cyan mutant) and acceptor (GFP^{S65T} or the yellowish mutant) fluorophores tethered through a connecting peptide that contains

cell coexpressing GFP-GRIP1 (*left*) and BFP-Pit-1 (*middle*). The merged GFP and BFP images demonstrate the distinct nuclear distribution patterns for these two fusion proteins. C, Images of the nuclei from two HeLa cells coexpressing the GFP-GRIP1 (*left*) and hER-BFP (*middle*) fusion proteins. The merged image shows a high degree of correspondence in the distribution patterns for these two fusion proteins (indicated by *yellow*).

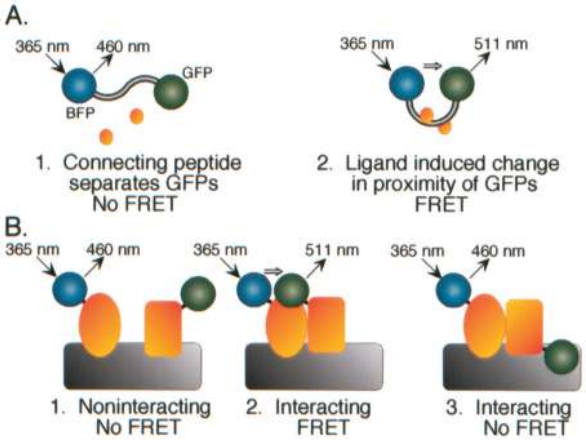

Fig. 2. Diagrammatic Representation of Intramolecular and Intermolecular FRET between Proteins Fused to the Color Variants of GFP

A, Scheme showing how intramolecular FRET between two color variants of GFP fused to one-another by a connecting peptide can serve as a biosensor for the binding of a ligand. In the absence of ligand the connecting peptides separates the GFPs beyond the critical distance required for energy transfer (1). Upon binding of ligand, a change in conformation of the connecting peptide can bring the GFPs within the proximity necessary for FRET, resulting in green light emission when BFP is excited (2). B, Scheme showing how intermolecular FRET between two independent proteins labeled with the GFPs can indicate protein-protein interactions. For noninteracting proteins (1), illumination of the cells to excite BFP (365 nm) results in emission of *blue* light (460 nm). In contrast, illumination of the cells expressing interacting fusion proteins can result in emission of *green* light (511 nm) because of FRET from BFP to GFP, an indication that the proteins are in physical contact (2). However, a negative result using the FRET technique does not indicated that the proteins fail to interact as illustrated in (3).

the binding site for another molecule (Fig. 2A). The interaction of the molecule with the connecting peptide induces a change in the relative position of the fluorophores and thus alters the FRET signal. Monitoring FRET signals from chimeric proteins containing a connecting peptide that binds calcium or calcium-calmodulin has proven to be a sensitive indicator of calcium homeostasis in living cells (51, 55). Moreover, the ability to target the expression of these fusion proteins to specific cellular organelles allows for the real-time monitoring of localized changes in calcium homeostasis in the intact cell (51). These studies illustrate the utility of intramolecular FRET as a reporter of dynamic intracellular events and predict the development of biosensors that will indicate a variety of activities in intact cells (56). A second FRET approach involves the detection of intermolecular interactions between two different protein partners labeled with the GFPs (Fig. 2B). In this case the labeled proteins are not limited in the distance they can be separated. Thus, the detection of sensitized fluorescence emission from pairs of proteins labeled with two different color variants of GFP can provide direct evidence for physical interactions between these proteins. This approach has the potential of being more generally applicable than intramolecular FRET in that it can be used to examine the interactions between many different classes of cellular proteins.

The results shown in Fig. 3 illustrate the acquisition of FRET signals from living cells using both the intramolecular and intermolecular approaches. In the first example, intramolecular FRET is detected from HeLa cells expressing a chimeric protein in which GFP is coupled to BFP through a nine- amino acid (AA) linker (Fig. 3A). The cells expressing the fusion protein were identified by green fluorescence. Donor and acceptor images were then acquired by first exciting BFP and detecting blue light emission (donor), and then by exciting BFP and detecting green light emission (acceptor) using the filter combinations described in the legend of Fig. 3. The background-subtracted donor and acceptor images are combined into a single mosaic image and a look-up table (LUT) is applied to indicate the pixel-by-pixel fluorescence signal intensity (Fig. 3A). To facilitate the direct comparison of signal levels, the gray level intensity for both donor and acceptor fluorescence across the profiles of the two cells shown in Fig. 3A was determined and the results are plotted. Comparison of nine similar cells expressing the GFP-9AA-BFP protein show that the average acceptor signal was 2.3-fold greater than the donor signal (*inset*, Fig. 3A). These results are consistent with the intramolecular transfer of BFP excitation energy to the tethered GFP yielding the emission of green light.

We reported previously the application of this FRET imaging approach to visualize the physical association of Pit-1 proteins labeled with GFP and BFP in the nucleus of living cells (38). Here we use the coexpression of these protein partners to illustrate the acquisition of intermolecular FRET signals. HeLa cells expressing the Pit-1 fusion proteins were first identified by green fluorescence (Fig. 3B). Donor and acceptor images of seven adjacent cells were then acquired using the same conditions described for the GFP-9AA-BFP protein. A mosaic of the background subtracted donor (BFP-Pit-1) and acceptor images was obtained and the same LUT was applied to indicate fluorescence intensity (Fig. 3B). Gray level intensity profiles across each of the nuclei shown in Fig. 3B were acquired and the results plotted. On average, the acceptor signals exceeded the donor signals by 1.6-fold (*inset*, Fig. 3B), indicating that energy transfer occurred from BFP-Pit-1 to GFP-Pit-1, requiring that these proteins be in physical contact.

A significant limitation to the FRET imaging approach is that the failure to detect sensitized green light emission from a pair of labeled proteins can not be interpreted as an indication that these proteins do not physically associate. For example, we have applied the FRET imaging approach to monitor the formation of partnerships between Pit-1 and other nuclear proteins, including the estrogen receptor (38). Cooperative interactions between Pit-1 and the estro-

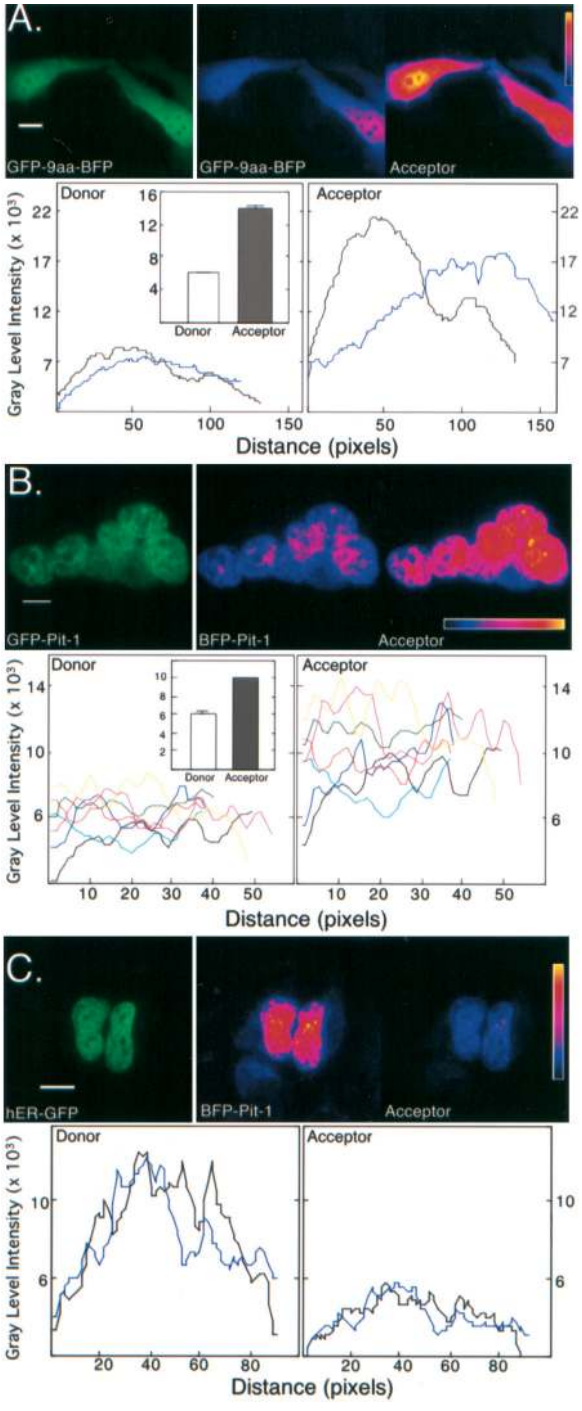

Fig. 3. FRET Microscopy of Living Cells Expressing GFP and BFP Fusion Proteins

Methods: The same GFP and BFP (donor) filter sets were used as described in the legend of Fig. 1; the acceptor (FRET) filter set is 365/15 nm excitation and 520/40 nm emission. FRET images were obtained using a slow scan, liquid nitrogen-cooled charge coupled device camera with a back-thinned, back-illuminated imaging chip (CH260, Photometrics). The digital image output of the camera is 512 × 512 pixels with 16 bits resolution. All donor and acceptor images were collected under identical conditions using a 5 sec on-chip integration time. All fluorescence signals fell within the range of 10 to 35 K gray level intensity (before background subtraction), and none of the images had saturated pixels. The Silicon Graphics, Inc. based ISEE software (Inovision Corporation, Raleigh, NC) was used to obtain the mosaic images and determine the gray level intensity profiles. A, Images of two HeLa cells expressing the GFP-9AA-BFP fusion protein were obtained using the GFP filter set (*left*; bar, 10 μm), BFP filter-set (*middle*) and the acceptor filter-set (*right*). The donor and acceptor images are combined in a single mosaic image and a LUT was applied to facilitate comparison of fluorescence signal intensity (calibration bar indicates signal level with *yellow* being highest intensity). A profile was taken across each cell and the gray level intensity for this profile was plotted for both the donor and acceptor images (*lower panels*). The average donor and acceptor signal gray level intensity determined for nine individual cells was then plotted ± SEM (*inset*). B, Images of HeLa cells were coexpressing the GFP-Pit-1 and BFP-Pit-1 proteins were obtained using the GFP filter set (*left*; bar, 10 μm), BFP filter set (*middle*) and the acceptor filter set (*right*), and a mosaic image of donor and acceptor fluorescence was acquired as described above. The gray level intensity profile across each of the cell nuclei was determined, and these profiles are plotted for both the donor and acceptor images (*lower panels*). The average donor and acceptor gray level intensity for the seven cells was determined and plotted ± SEM (*inset*). C, HeLa cells coexpressing the hER-GFP and BFP-Pit-1 proteins were maintained in medium supplemented with 10% newborn calf serum containing endogenous estrogens. Images were obtained using the GFP filter-set (*left*; bar, 10 μm), BFP filter set and the acceptor filter set. The mosaic image of donor and acceptor fluorescence was acquired, and the gray level intensity profile across the two cell nuclei is plotted for both the donor and acceptor images (*lower panels*). The data in panel C are reproduced from Ref. 38 with permission.

gen receptor are a key step in the regulation of PRL gene transcription, and a physical association of these two proteins was demonstrated by *in vitro* techniques (57, 58). The results in Fig. 3C show FRET imaging of HeLa cells coexpressing the human estrogen receptor labeled with GFP (hER-GFP) and the BFP-Pit-1 fusion protein. The mosaic showing the background-subtracted donor (BFP-Pit-1) and acceptor (hER-GFP) images reveals that the pixel-by-pixel fluorescence intensity for the acceptor image is significantly less than that of the donor image. The gray level intensity profile across the two nuclei shown in Fig. 3C confirms that the acceptor signal is approximately 2-fold lower than the donor signal. These results are similar to those obtained for colocalized, but noninteracting, proteins labeled with the GFPs (38).

There are many potential reasons why interacting protein partners may fail to produce FRET signals. Energy transfer is dependent not only upon the distance separating the fluorophores, but upon their orientation as well (59). In the case of proteins labeled with the GFPs, the fluorophores are positioned at the ends of the potentially interacting proteins. The conformations that are adopted by the proteins when they associate may not allow the fluorophores to be in close enough proximity or to align appropriately for

energy transfer to occur (see Fig. 2B). Further, the endogenous counterparts of the labeled proteins will also interact with the expressed GFP chimeras, competing for potential productive interactions. This can be minimized by expressing the labeled proteins in heterologous cell types that lack the endogenous proteins, or by expressing the labeled protein partners in excess of the endogenous proteins. However, excessively high level expression of proteins that are localized similarly within the cell, but not directly interacting, could potentially allow FRET to occur by diffusion. As with any approach involving the expression of proteins in living cells, artifacts that arise from overexpression of the fusion proteins are a concern. Control experiments with labeled proteins that colocalize, but that should not physically interact, can be used to assess the contribution of diffusion to measured FRET signals.

A further limitation of FRET microscopy, especially when performed with two independent proteins in the context of living cells, is the challenge of accounting for spectral cross-talk for both the donor and acceptor fluorophores. This occurs when the donor emission overlaps into the acceptor filter and when the acceptor emission occurs at the donor excitation wavelengths. The result of spectral cross-talk is a high and variable background against which FRET signals must be compared. The detection of intermolecular FRET using the GFPs is also limited by the uncertainty of the absolute concentrations of the expressed donor and acceptor fusion proteins. Therefore, meticulous attention to a consistent protocol for image collection is necessary to obtain meaningful data. Recently, a quantitative method for determining FRET efficiency was introduced (60). This method enhances the sensitivity of FRET measurements by correcting for the cross-talk for donor and acceptor pairs, even when they exhibit substantial spectral overlap. This approach was used by Mahajan and colleagues (61) to examine protein-protein interactions between two proteins involved in the regulation of apoptosis, Bcl-2 and Bax. Dual-channel fluorescence microscopy revealed that the BFP-Bcl-2 and GFP-Bax proteins are colocalized to the mitochondria, and quantitative FRET demonstrated that these proteins formed heterodimers.

OVERVIEW AND CONCLUSIONS

Currently, yeast two-hybrid assay is the method of choice for identifying interacting protein partners. However, not all protein partnerships indicated by yeast two-hybrid screening represent true physiological interactions. The verification that these protein partners interact in a meaningful way *in vivo* can be difficult to demonstrate. FRET provides a potentially invaluable methodological asset to confirm these protein-protein interactions in the intact cell. The potential for FRET microscopy of living cells expressing labeled fusion proteins has only just begun to be realized. New approaches are being developed that utilize different energy transfer partners for GFP that may significantly improve the detection of protein interactions. For example, Griffin and colleagues (62) have developed a fluorescent label called FLASH-EDT2 that can cross cell membranes and covalently bind to recombinant proteins that are tagged with a short 17-AA peptide containing the core tetracysteine motif CCXXCC. The FLASH-EDT2 is virtually nonfluorescent, but becomes becomes brightly fluorescent when it binds to the tetracysteine peptide. Its excitation and emission spectra make it suitable as an acceptor of excitation energy from the cyan mutant of GFP. The ability to add the acceptor fluorophore to cells already expressing the donor provides a particularly useful control for FRET, in that the donor signal can be quantified first in the absence, and then in the presence of the acceptor fluorophore (62). A second novel approach takes advantage of the naturally occurring energy transfer system used by the jellyfish *Aequorea*. In the jellyfish, the calcium-binding photoprotein aequorin emits blue light that excites green light emission from GFP. Studies by Xu *et al*. (63) have demonstrated that resonance energy transfer between the bioluminescent *Renilla* luciferase and yellowish color variant of GFP, referred to as bioluminescence resonance energy transfer (BRET), may have several advantages over the fluorescence-based FRET approach. Because the donor is a luciferase, spectral cross-talk, photobleaching, and autofluorescence are not a concern in using the BRET approach. The authors have applied the BRET approach to demonstrate the formation of homodimers involving the cyanobacteria circadian clock protein KaiB in *Escherichia coli*. These recent developments anticipate further technical improvements in the combined use of GFP-labeled proteins and FRET microscopy. For many important physiological processes, such as the regulation of transcription by the nuclear receptors and their coregulatory partners, the critical events are coordinated in space and time through sequential, but transient, interactions within complex macromolecular assemblies. The power of the FRET approach is in the detection of these intricate social behaviors between regulatory proteins in their natural environment within the living cell.

Acknowledgments

Much of the information presented in this paper is the result of discussions with our colleagues Steve Kay, Shelley Halpain, and David Brautigan. The authors wish to thank Ammasi Periasamy of the Center for Cellular Imaging at the University of Virginia for his help. We are grateful to Michael Stallcup for supplying the cDNA encoding GRIP1 and acknowledge the expert technical assistance of Margaret Kawecki.

Received November 13, 1998. Re-revision received December 18, 1998. Accepted December 21, 1998.

Address requests for reprints to: Richard N. Day, Ph.D., Department of Internal Medicine, Box 578, University of

Virginia Health Sciences Center, Charlottesville, Virginia 22903 E-mail: rnd2v@virginia.edu

This study was supported by National Science Foundation Grant DIR-8920162, Center for Biological Timing Technology Development subproject (R.N.D.), NIH Grant RO1-DK-43701 (R.N.D.), and NIH Grant RO1 DK-37061 (S.K.N.).

REFERENCES

1. Pratt WB, Toft DO 1997 Steroid receptor interactions with heat shock protein and immunophilin chaperones. Endocr Rev 18:306–360
2. Horwitz KB, Jackson TA, Bain DL, Richer JK, Takimoto GS, Tung L 1996 Nuclear receptor coactivators and corepressors. Mol Endocrinol 10:1167–1177
3. Glass CK, Rose DW, Rosenfeld MG 1997 Nuclear receptor coactivators. Curr Opin Cell Biol 9:222–232
4. Shibata H, Spencer TE, Onate SA, Jenster G, Tsai SY, Tsai MJ, O'Malley BW 1997 Role of co-activators and co-repressors in the mechanism of steroid/thyroid receptor action. Recent Prog Horm Res 52:141–164
5. Prasher DC, Eckenrode VK, Ward WW, Prendergast FG, Cormier MJ 1992 Primary structure of the *Aequorea victoria* green-fluorescent protein. Gene 111:229–233
6. Chalfie M, Tu Y, Euskirchen G, Ward WW, Prasher DC 1994 Green fluorescent protein as a marker for gene expression. Science 263:802–805
7. Niswender KD, Blackman SM, Rohde L, Magnuson MA, Piston DW 1995 Quantitative imaging of green fluorescent protein in cultured cells: comparison of microscopic techniques, use in fusion proteins and detection limits. J Microsc 180:109–116
8. Plautz JD, Day RN, Dailey GM, Welsh SB, Hall JC, Halpain S, Kay SA 1996 Green fluorescent protein and its derivatives as versatile markers for gene expression in living *Drosophila melanogaster*, plant and mammalian cells. Gene 173:83–87
9. Gerdes HH, Kaether C 1996 Green fluorescent protein: applications in cell biology. FEBS Lett 389:44–47
10. Misteli T, Spector DL 1997 Applications of the green fluorescent protein in cell biology and biotechnology. Nat Biotechnol 15:961–964
11. Carey KL, Richards SA, Lounsbury KM, Macara IG 1996 Evidence using a green fluorescent protein-glucocorticoid receptor chimera that the Ran/TC4 GTPase mediates an essential function independent of nuclear protein import. J Cell Biol 133:985–996
12. Htun H, Barsony J, Renyi I, Gould DL, Hager GL 1996 Visualization of glucocorticoid receptor translocation and intranuclear organization in living cells with a green fluorescent protein chimera. Proc Natl Acad Sci USA 93:4845–4850
13. Georget V, Lobaccaro JM, Terouanne B, Mangeat P, Nicolas JC, Sultan C 1997 Trafficking of the androgen receptor in living cells with fused green fluorescent protein-androgen receptor. Mol Cell Endocrinol 129: 17–26
14. Presley JF, Cole NB, Schroer TA, Hirschberg K, Zaal KJ, Lippincott-Schwartz J 1997 ER-to-Golgi transport visualized in living cells. Nature 389:81–85
15. Wacker I, Kaether C, Kromer A, Migala A, Almers W, Gerdes HH 1997 Microtubule-dependent transport of secretory vesicles visualized in real time with a GFP-tagged secretory protein. J Cell Sci 110:1453–1463
16. Kaether C, Salm T, Glombik M, Almers W, Gerdes HH 1997 Targeting of green fluorescent protein to neuroendocrine secretory granules: a new tool for real time studies of regulated protein secretion. Eur J Cell Biol 74:133–142
17. Barak LS, Ferguson SS, Zhang J, Caron MG 1997 A beta-arrestin/green fluorescent protein biosensor for detecting G protein-coupled receptor activation. J Biol Chem 272:27497–27500
18. Wu P, Brand L 1994 Resonance energy transfer: methods and applications. Anal Biochem 218:1–13
19. Heim R, Prasher DC, Tsien RY 1994 Wavelength mutations and posttranslational autoxidation of green fluorescent protein. Proc Natl Acad Sci USA 91:12501–12504
20. Inouye S, Tsuji FI 1994 Evidence for redox forms of the *Aequorea* green fluorescent protein. FEBS Lett 351:211–214
21. Brejc K, Soxma TK, Kitts PA, Kain SR, Tsien RY, Remington SJ 1997 Structural basis for dual excitation and photoisomerization of the *Aequorea victoria* green fluorescent protein. Proc Natl Acad Sci USA 94:2306–2311
22. Reid BG, Flynn GC 1997 Chromophore formation in green fluorescent protein. Biochemistry 36:6786–6791
23. Ormö M, Cubitt, AB, Kallio K, Gross LA, Tsien RY, Remington SJ 1996 Crystal structure of the *Aequorea victoria* green fluorescent protein. Science 273:1392–1395
24. Dopf J, Horiagon TM 1996 Deletion mapping of the *Aequorea victoria* green fluorescent protein. Gene 173: 39–44
25. Heim R, Cubitt AB, Tsien RY 1995 Improved green fluorescence. Nature 373:663–664
26. Patterson GH, Knobel SM, Sharif WD, Kain SR, Piston DW 1997 Use of the green fluorescent protein and its mutants in quantitative fluorescence microscopy. Biophys J 73:2782–2790
27. Aubin JE 1979 Autofluorescence of viable cultured mammalian cells. J Histochem Cytochem 27:36–43
28. Zhuo L, Sun B, Zhang CL, Fine A, Chiu SY, Messing A 1997 Live astrocytes visualized by green fluorescent protein in transgenic mice. Dev Biol 187:36–42
29. Heim R, Tsien RY 1996 Engineering green fluorescent protein for improved brightness, longer wavelengths and fluorescence resonance energy transfer. Curr Biol 6:178–182
30. Chiu W, Niwa Y, Zeng W, Hirano T, Kobayashi H, Sheen J 1996 Engineered GFP as a vital reporter in plants. Curr Biol 6:325–330
31. Yang TT, Cheng L, Kain SR 1996 Optimized codon usage and chromophore mutations provide enhanced sensitivity with the green fluorescent protein. Nucleic Acids Res 24:4592–4593
32. Zolotukhin S, Potter M, Hauswirth WW, Guy J, Muzyczka N 1996 A "Humanized" green fluorescent protein cDNA adapted for high-level expression in mammalian cells. J Virol 70:4646–4654
33. Kimata Y, Iwaki, M, Lim, CR, Kohno K 1997 A novel mutation which enhances the fluorescence of green fluorescent protein at high temperatures. Biochem Biophys Res Commun 232:69–73
34. Siemering EM, Golbik R, Sever R, Haseloff J 1996 Mutations that suppress the thermosensitivity of green fluorescent protein. Curr Biol 6:1653–1663
35. Rizzuto R, Brini M, De Giorgi F, Rossi R, Heim R, Tsien RY, Pozzan T 1996 Double labeling of subcellular structures with organelle-targeted GFP mutants *in vivo*. Curr Biol 6:183–188
36. Yang TT, Sinai P, Green G, Kitts PA, Chen YT, Lybarger L, Chervenak R, Patterson GH, Piston DW, Kain SR 1998 Improved fluorescence and dual color detection with enhanced blue and green variants of the green fluorescent protein. J Biol Chem 273:8212–8216
37. Wang S, Hazelrigg T 1994 Implications for bcd mRNA localization from spatial distribution of exu protein in *Drosophila* oogenesis. Nature 369:400–403
38. Day RN 1998 Visualization of Pit-1 transcription factor interactions in the living cell nucleus by fluorescence resonance energy transfer microscopy. Mol Endocrinol 12:1410–1419
39. Take-Uchi M, Kawakami M, Ishihara T, Amano T, Kondo K, Katsura I 1998 An ion channel of the degenerin/epi-

thelial sodium channel superfamily controls the defecation rhythm in *Caenorhabditis elegans*. Proc Natl Acad Sci USA 95:11775–11780
40. Dunn K, Maxfield FR 1998 Ratio imaging instrumentation. Methods Cell Biol 56:217–236
41. Periasamy A, Day RN 1998 Visualizing protein interactions in living cells using digitized GFP imaging and FRET microscopy. Methods Cell Biol 58:293–313
42. Stein GS, van Wijnen AJ, Stein JL, Lian JB, Pockwinse S, McNeil SJ 1998 Interrelationships of nuclear structure and transcriptional control: functional consequences of being in the right place at the right time. Cell Biochem 70:200–212
43. van Steensel B, van Binnendijk EP, Hornsby CD, van der Voort HT, Krozowski ZS, de Kloet ER, van Driel R 1996 Partial colocalization of glucocorticoid and mineralocorticoid receptors in discrete compartments in nuclei of rat hippocampus neurons. J Cell Sci 109:787–92
44. Fejes-Toth G, Pearce D, Naray-Fejes-Toth A 1998 Subcellular localization of mineralocorticoid receptors in living cells: effects of receptor agonists and antagonists. Proc Natl Acad Sci USA 95:2973–2978
45. Hager GL, Smith CL, Fragoso G, Wolford R, Walker D, Barsony J, Htun H 1998 Intranuclear trafficking and gene targeting by members of the steroid/nuclear receptor superfamily. J Steroid Biochem Mol Biol 65:125–132
46. Voegel JJ, Heine MJ, Zechel C, Chambon P, Gronemeyer H 1996 TIF2, a 160 kDa transcriptional mediator for the ligand-dependent activation function AF-2 of nuclear receptors. EMBO J 15:3667–3675
47. Hong H, Kohli K, Garabedian MJ, Stallcup MR 1997 GRIP1, a transcriptional coactivator for the AF-2 transactivation domain of steroid, thyroid, retinoid, and vitamin D receptors. Mol Cell Biol 17:2735–2744
48. Norris JD, Fan D, Stallcup MR, McDonnell DP 1998 Enhancement of estrogen receptor transcriptional activity by the coactivator GRIP-1 highlights the role of activation function 2 in determining estrogen receptor pharmacology. J Biol Chem 273:6679–6688
49. Cubitt AB, Heim R, Adams SR, Boyd AE, Gross LA, Tsien RY 1995 Understanding, improving and using green fluorescent proteins. Trends Biochem Sci 20:448–455
50. Mitra RD, Silva CM, Youvan DC 1996 Fluorescence resonance energy transfer between blue-emitting and redshifted excitation derivatives of the green fluorescent protein. Gene 173:13–17
51. Miyawaki A, Llopis J, Heim R, McCaffery JM, Adams JA, Ikura M, Tsien RY (1997) Fluorescent indicators for Ca2+ based on green fluorescent proteins and calmodulin. Nature 388:882–887
52. Kubitscheck U, Schweitzer-Stenner R, Arndt-Jovin DJ, Jovin TM, Pecht I 1993 Distribution of type I Fc epsilon-receptors on the surface of mast cells probed by fluorescence resonance energy transfer. Biophys J 64:110–120
53. Guo C, Dower SK, Holowka D, Baird B 1995 Fluorescence resonance energy transfer reveals interleukin (IL)-1-dependent aggregation of IL-1 type I receptors that correlates with receptor activation. J Biol Chem 270: 27562–27568
54. Bacskai BJ, Hochner B, Mahaut-Smith M, Adams, SR, Kaang BK, Kandel ER, Tsien RY 1993 Spatially resolved dynamics of cAMP and protein kinase A subunits in Aplysia sensory neurons. Science 260:222–226
55. Romoser VA, Hinkle PM, Persechini A 1997 Detection in living cells of Ca2+-dependent changes in the fluorescence emission of an indication composed of two green fluorescent protein variants linked by a calmodulin-binding sequence: a new class of fluorescent indicators. J Biol Chem 272:13270–13274
56. Tsien RY, Miyawaki A 1998 Seeing the machinery of live cells. Science 280:1954–1955
57. Day RN, Koike S, Sakai M, Muramatsu M, Maurer RA (1990) Both Pit- 1 and the estrogen receptor are required for estrogen responsiveness of the rat PRL gene. Mol Endocrinol 4:1964–1971
58. Nowakowski BE, Maurer RA (1994) Multiple Pit-1-binding sites facilitate estrogen responsiveness of the prolactin gene. Mol Endocrinol 8:1742–1749
59. dos Remedios CG, Moens PDJ 1995 Fluorescence resonance energy transfer spectroscopy is a reliable "ruler" for measuring structural changes in proteins. Dispelling the problem of the unknown orientation factor. J Struct Biol 115:175–185
60. Gordon GW, Berry G, Liang XH, Levine B, Herman B 1998 Quantitative fluorescence resonance energy transfer measurements using fluorescence microscopy. Biophys J 74:2702–2713
61. Mahajan NP, Linder K, Berry G, Gordon GW, Heim R, Herman B 1998 Bcl-2 and Bax interactions in mitochondria probed with green fluorescent protein and fluorescence resonance energy transfer. Nat Biotechnol 16: 547–552
62. Griffin BA, Adams SR, Tsien RY 1998 Specific covalent labeling of recombinant protein molecules inside living cells. Science 281:269–272
63. Xu Y, Piston DW, Johnson CH 1998 A novel bioluminescence resonance energy transfer (BRET) system: application to interacting of circadian clock proteins. Proc Natl Acad Sci USA 96:151–156